

## Direct Measurement of the Total Light of Rapidly Decaying Processes of Luminescence

N. A. TOLSTOI AND I. A. LITVINENKO

(Submitted to JETP editor June 13, 1954)

J. Exper. Theoret. Phys. USSR 29, 507-515 (October, 1955)

A new, objective method is proposed for the direct measurement of  $L_p$  and  $L_z$  for rapidly proceeding luminescent processes.

The relationship of the area above the curve of fluorescent rise  $L_p$  to the area under the curve of fluorescent decay  $L_z$  can serve as the criterion for the selection of one or another theory of phosphorescence, since the various theories, generally speaking, predict different magnitudes for  $L_p/L_z$ . The measurement of  $L_p/L_z$  for a quenched ZnS-Cu phosphor indicates the inapplicability of a theory based on a bimolecular mechanism of luminescence and a monomolecular mechanism of decay.

### 1. INTRODUCTION

AS experience in the study of the kinetics of the processes of luminescence<sup>1,2</sup> shows, the relaxation curves for luminescence, with the exception of a small number of "favorable" cases, cannot, as a rule, be described to any extent by simple analytic laws\*.

The complexity of the laws of relaxation in crystalline phosphors makes the task of qualitative integration of the relaxation curves extremely difficult. In this connection it is expedient in a number of instances to make the object of the investigation not the relaxation curves themselves, but rather several simpler quantities, which are in the final analysis connected with the form of the relaxation curves. Thus, for example, the method of electrical differentiation<sup>4</sup> makes it possible to measure the slope of the luminescent decay curve or the curve of the drop in photoconductivity at an instant of time directly following the instant of departure of the system from the stationary state. The measurement of this slope results in a number, characterizing "the departure of the system from the stationary condition".

Utilization of this method makes it possible to

draw important conclusions as to the nature of the luminescence of crystalline phosphors and the nature of photoconductivity.

It is possible to indicate another magnitude, expressed by a single number, which is closely related to the form of the relaxation curve—specifically, the integral of the luminescent decay curve

$$L_z = \int_0^{\infty} I_z(t) dt,$$

and also the magnitude

$$L_p = \int_0^{\infty} (I_{\text{stat}} - I_p(t)) dt.$$

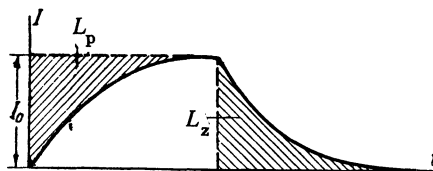


FIG. 1. Geometric significance of the magnitudes  $L_p$  and  $L_z$ .

\* In this article we shall deal only with "rapid" processes of luminescent rise and decay ( $10^{-1}$  to  $10^{-5}$  sec), i.e., with luminophors, the relaxation curves of which can be studied by the Tau-meter method<sup>3</sup>.

<sup>1</sup> V. S. Arkhangel'skaia, A. M. Bonch-Bruevich, N. A. Tolstoi and P. P. Feofilov, J. Exper. Theoret. Phys. USSR 21, 290 (1951).

<sup>2</sup> N. A. Tolstoi and P. P. Feofilov, Izv. Akad. Nauk SSSR, Ser. Fiz. 16, 59 (1952).

<sup>3</sup> N. A. Tolstoi and P. P. Feofilov, Uspekhi Fiz. Nauk 41, 44 (1950).

<sup>4</sup> N. A. Tolstoi, Izv. Akad. Nauk SSSR, Ser. Fiz. 15, 690 (1951).

Figure 1 demonstrates the geometric meaning of the magnitudes  $L_z$  and  $L_p$ . Each of these is equal to the corresponding cross-hatched area.

The present article deals with the problem of the measurement of the magnitudes  $L_z$  and  $L_p$ . It may be noted here that a study of the magnitude  $L_z$ , corresponding to prolonged processes of phosphorescence (minutes, hours), was carried out as long as half a century ago by means of the graphic integration of decay curves, recorded point by point with the aid of a stop watch. The measure-

ment of  $L_z$  and also of  $L_p$  for the initial stages of relaxation (from  $10^{-5}$  to  $10^{-1}$  sec) has never been made by anyone up to the present time.

## 2. THE RELATIONSHIPS OF THE MAGNITUDES

### $L_p$ AND $L_z$ FOR SEVERAL CASES

a) Let us imagine a luminophor in which no decay exists, i.e., in which every excited electron returns to the unexcited condition by emitting one quantum of luminescence. Then, hypothesizing that each quantum of excited light excites one electron, it is possible to write the most general kinetic equation

$$dn/dt = -I(n) + E, \quad (1)$$

where  $n$  is the number of excited electrons,  $I$  is the number of emissive transitions per second and  $E$  is the number of quanta of excitational light absorbed in one second by the luminophor. The solution of (1) results in curves of fluorescent decay and rise,  $I_z(t)$  and  $I_p(t)$ , which depend parametrically on  $E$ . We will consider that  $E = \text{constant}$  or that  $E = 0$ , i.e., we will examine, as usual, "square wave" excitation. Then

$$I_z(0) = E, \quad I_z(\infty) = 0, \quad I_p(0) = 0, \quad I_p(\infty) = E$$

and

$$\int_0^{n_\infty} dn = \int_0^\infty (E - I_p(t)) dt = L_p,$$

$$-\int_{n_\infty}^0 dn = \int_0^\infty I_z(t) dt = L_z,$$

From whence

$$L_p = L_z. \quad (2)$$

In this case  $L_p$  has the significance of the total stored light, and  $L_z$  the total light emitted during the decay process. Since no hypothesis has been made with regard to the form of the function  $I(n)$ , it is clear that Eq. (2) is valid for any kinetics satisfying Eq. (1), in particular, for monomolecular, pseudomonomolecular and bimolecular kinetics.

b) If there is inactive absorption, i.e., if not every quantum of excitational light excites an electron (output  $< I$ , but no decay), Eq. (2) remains as before.

c) If there is decay after recombination, then Eq. (2) remains valid.

d) If there is decay before recombination and the kinetics of luminescence are monomolecular ( $I = \alpha n$ ),

$$dn/dt = -\alpha n - \beta n + \gamma E,$$

then Eq. (2) is valid.

e) If there is decay before recombination and the kinetics of luminescence are bimolecular ( $I = \alpha n^2$ ),

$$dn/dt = -\alpha n^2 - \beta n + \gamma E,$$

then in the limiting case of very rapid decay ( $\beta n \gg \alpha n^2$ )

$$I = \frac{\gamma^2 E^2}{\beta^2} (1 - e^{-\beta t})^2 \quad (\text{rise}),$$

$$I = \frac{\gamma^2 E^2}{\beta^2} e^{-2\beta t} \quad (\text{decay})$$

and  $L_p = 3L_z$ .

Since in the other limiting case (vanishingly small decay)  $L_p = L_z$ , then the intermediate cases lie within the limits

$$L_z \ll L_p \ll 3L_z.$$

f) If there is no decay, but an extinguishing action takes place on the part of the exciting light, then

$$L_p < L_z.$$

The foregoing examples are adequate to convince one that the ratio  $L_p/L_z$  can serve as one of the criteria for judging the applicability of one or another mechanism for the interpretation of the kinetics of luminescent rise or decay\*. The selection of concrete models, of course, results in a quantitative value for the magnitude  $L_p/L_z$ , which can be checked by experiment.

### 3. L-METER

The task described in the introduction is, from the point of view of methodology, related to the measurement of the area above the luminescence rise curve  $L_p$  and the area under the luminescence decay curve  $L_z$  (Fig. 1) by electronic means. Since the rise and decay curves under study represent electrical signals which do not possess a constant component due to the method by which

\* A more-detailed analysis of the connection between the magnitude  $L_p/L_z$  and the character of the kinetics will be given in a later publication.

they are obtained (passage through a circuit having dividing capacitors--see Fig. 2, *a*) the integral of these curves on the whole is equal to zero. The artificial introduction of a constant component corresponding to the zero reading at complete decay (Fig. 2, *b*) permits us to obtain the integral of the decay curve. However, it is obtained simultaneously and inseparably with the integral under the rise curve which does not interest us. It is obvious that in order to perform our task it is necessary to change the investigated signal in such a manner as to remove from the signal--in the one case, the rise curve (Fig. 2, *c*), and in the other case, the decay curve (Fig. 2, *d*). In the first case the integral will be positive and proportional to  $L_z$ , and in the second case, negative and proportional to  $L_p$ .

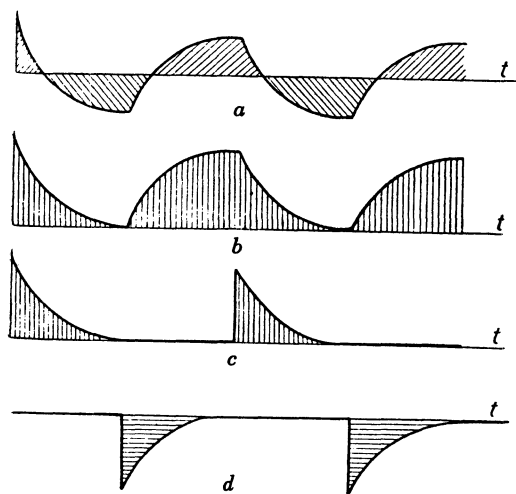


FIG. 2. *a*. Signal after passing through a divider circuit; *b*. The same signal with the addition of a constant component producing a zero reading corresponding to complete decay; *c*. Rise curve eliminated, zero reading is at complete decay; *d*. Decay curve eliminated, zero reading is at complete rise.

If the aforementioned transformation of the signal (the displacement of the zero line and the elimination of one or another half of the curves) is accomplished, then it is possible to solve the given problem by integration of the signals with the aid of any electrical measuring instrument which possesses sufficient inertia (the natural period of the instrument should be much greater than the period of repetition of the signals) and which will respond to the average value of the voltage or current (for example, a needle-indicating magneto-electric microammeter). The basic method with the aid of which we obtain the desired transformation of the signal consists in the

application of synchronized detection. The signal controlling the operation of the synchronized detector is in the final analysis a rectangular light pulse (square wave) synchronized with the square wave of light which excites luminescence in the luminophor being investigated.

#### 4. OPTICAL SETUP

The schematic for obtaining square waves of light and transforming the luminescence relaxation curves into corresponding electrical signals fully conforms to the schematic of the Tau-meter<sup>3</sup> which is based on the mechanical modulation of light, with the sole difference that in our setup there is no functional analysis. Since the Tau-meter has been described in detail in the works of Tolstoi and Feofilov, we will only briefly touch upon the optical portions of the method.

As can be seen from Fig. 3, the excitational light from a mercury arc lamp  $L_1$  is focused on a narrow slit  $S_1$  near which the light beam is interrupted by the rotating disc  $D$ , which is equipped with projections. The square pulse of light thus obtained excites a sample of the luminophor  $O$ . The luminescence of the latter is detected by a photoelectric multiplier  $FEU-1$ , which is equipped with a cathode follower  $CF-1$ .  $K_1, K_2$  and  $K_3$  are condensing lenses;  $F_1$  and  $F_2$  are crossed polarizers. The second light source  $L_2$  produces synchronous square waves of light which are detected by  $FEU-2$  and repeated by  $CF-2$ . Thus, at the output of  $CF-1$ , relaxation curves are obtained which are the subject of investigation, and at the output of  $CF-2$  electrical square waves occur which control the process of synchronous detection. The steepness of the wave fronts of the square pulses in such a setup can be carried to  $10^{-5}$  sec. The repetition frequency of the square waves is 10-200 pulses/sec.

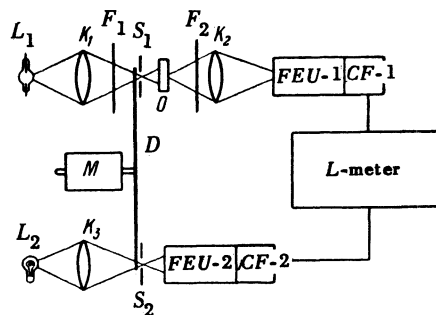


FIG. 3. Schematic of the optical setup.

#### 5. SYNCHRONOUS DETECTOR

The operation of the synchronous detector (*SD*)

is apparent from an examination of the schematic represented in Fig. 4. A duo-triode 6N8 (let us call it a synchronous signal detector) has two inputs 1 and 2, upon which are imposed, respectively, the square waves and the relaxation signals under investigation. Both halves of the tube have a common cathode resistance. The left-hand triode is a cathode follower; the right-hand triode is an amplifier with a cathode-anode load (i.e., with negative feedback). When the voltage on the grid of the left-hand triode is negative, the right-hand triode amplifies the signal and its plate voltage reproduces, let us say, the decay

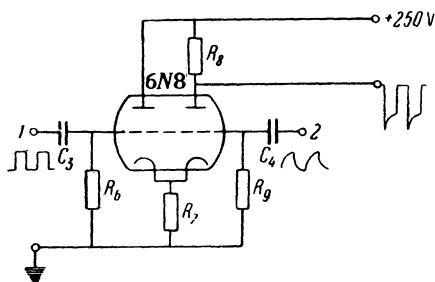


FIG. 4. Schematic of synchronous detector (for the values of  $R$  and  $C$ , see the subscript to Fig. 8).

curve (inverted, of course, as a result of the usual phase reversal in an amplifier stage with a plate load). When the voltage on the grid of the left-hand triode is positive and sufficiently large, a strong current flows in the cathode resistor, and the voltage drop across the resistor cuts off the right-hand triode completely. Instead of the "rise curve", a constant voltage appears at the plate of the right-hand triode which is equal to the B-plus voltage shown in the schematic. On the whole, the plate voltage of the right-hand triode has the appearance shown in Fig. 5, *a*. The rise curves have been eliminated, but in their place have appeared rectangular "projections". A second, completely analogous duo-triode (synchronous square wave detector) is used to eliminate these projections. Square waves of small, regulated amplitude are imposed on the grid of the right-hand triode, and controlling square waves of sufficiently large amplitude are imposed on the grid of the left-hand triode. At the plate of the right-hand triode, square waves are obtained with an upper voltage limit equal to the B-plus voltage (Fig. 5, *b*) and with an amplitude of  $\Delta V$ , which (with the aid of potentiometer  $A_3$ , see Fig. 8) is set equal to the  $\Delta V$  in

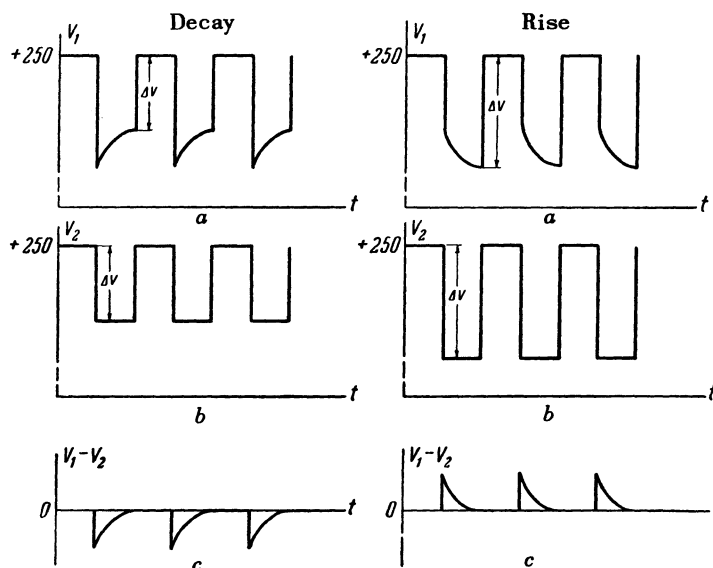


FIG. 5.- *a*. Voltage at the plate of the right-hand triode of the synchronous signal detector; *b*. Voltage at the plate of the right-hand triode of the synchronous square wave detector; *c*. Difference in the signals at the plates of the right-hand triodes of the synchronous signal detector and the synchronous square wave detector.

Fig. 5, *a*. (For the method of matching these voltages, see text following.) The difference between the two signals will then give a pure decay

curve computed from a zero base, and a pure zero line in place of the rise curve. (The "zero" in our instance will be the constant B-plus volt-

age.) The same figure shows the analogous treatment of the signal for obtaining a pure rise curve, which does not need further explanation.

If the signals at the plates of the right-hand triodes of the synchronous signal detector and the synchronous square wave detector are sufficiently strong, and if a microammeter connecting these anodes (in the form of a bridge) has a sufficiently high resistance, then the reading of the microammeter will be proportional to the area of the relaxation curve in which we are interested.

As we already stated, the square waves at the plate of the right-hand triode of the synchronous square wave detector are so adjusted that their amplitude  $\Delta V$  exactly "fills" the rectangular projection in the investigated relaxation curves, which are obtained as a result of the elimination of the undesirable halves of the processes in the

synchronous signal detector. Obviously, it is necessary to be able to control the correctness of this adjustment. To achieve this aim, a pulse shaper (*KFK*) is utilized. The schematic of the *KFK* unit is presented in Fig. 6, *a*. Signals from the synchronous signal detector (input 1) and the synchronous square wave detector (input 2) are impressed on the grids of the corresponding cathode followers, which are assembled in the single envelope of the duo-triode 6N8. An oscilloscope which is connected between the cathode outputs of the two followers reproduces the shape of the curve to be integrated. Regulation of the amplitude of the square wave "filler" projections can be attained by "compensation" (Fig. 6, *b*). If compensation is attained, integration of the curve will give the correct result being sought.

Since there is no *a priori* guarantee that the

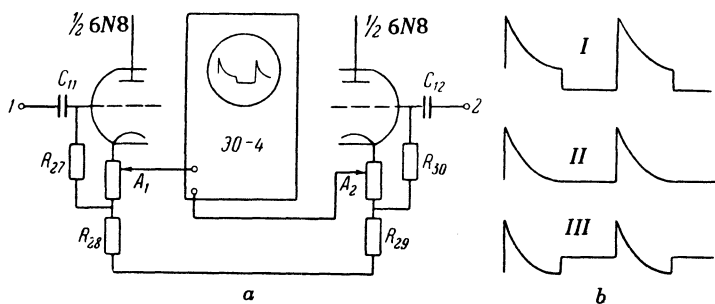


FIG. 6. *a*. Schematic of pulse shaper (*KFK*); *b*. Shape of the curves on the oscilloscope screen\* (for the values of  $R$  and  $C$ , see the subscript to Fig. 8): *I*, Insufficiently compensated; *II*, Compensated; *III*, Over-compensated.

operation of the two cathode followers will be identical, potentiometers  $A_1$  and  $A_2$  have been introduced in the circuit of the *KFK* unit (Fig. 6, *a*), by regulation of which complete symmetry of the circuit is attained. It is necessary, however,

to have some means of assuring ourselves that this symmetry is actually attained, i.e., that the *KFK* unit is itself working properly. To accomplish this, a pulse shaper control is employed. Instead of the relaxation curve being studied, square

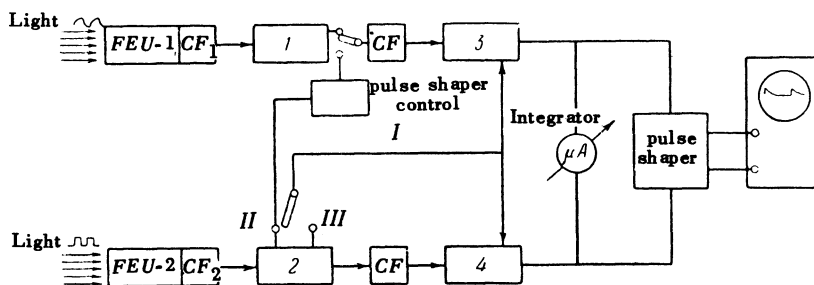


FIG. 7. Block diagram of the *L*-meter. 1. Signal amplifier; 2. Square wave amplifier; 3. Synchronous signal detector; 4. Synchronous square wave detector; *I*. Detected signal; *II*. Direct phase; *III*. Inverse phase.

control waves are imposed on the synchronous signal detector. It is clear that  $L_p$  and  $L_z$  for the square waves are equal to zero. Then, by regulation of the amplitude of these square control waves (potentiometer  $A_4$ , Fig. 8) or by regulation of the amplitude of the square waves obtained from the output of the synchronous square wave detector, we can attain a condition in which the integrating unit will produce a zero reading. This obviously corresponds to a condition in which the

voltage is always equal to zero and there are no "projections" between the output plates of the synchronous signal detector and the synchronous square wave detector. Then by regulation of potentiometers  $A_1$  and  $A_2$  in the *KFK* unit, we attain a condition in which a straight line without any "projections" is obtained on the oscilloscope screen. After this operation, the *KFK* unit may be considered adjusted, and the *L*-meter is ready for use.

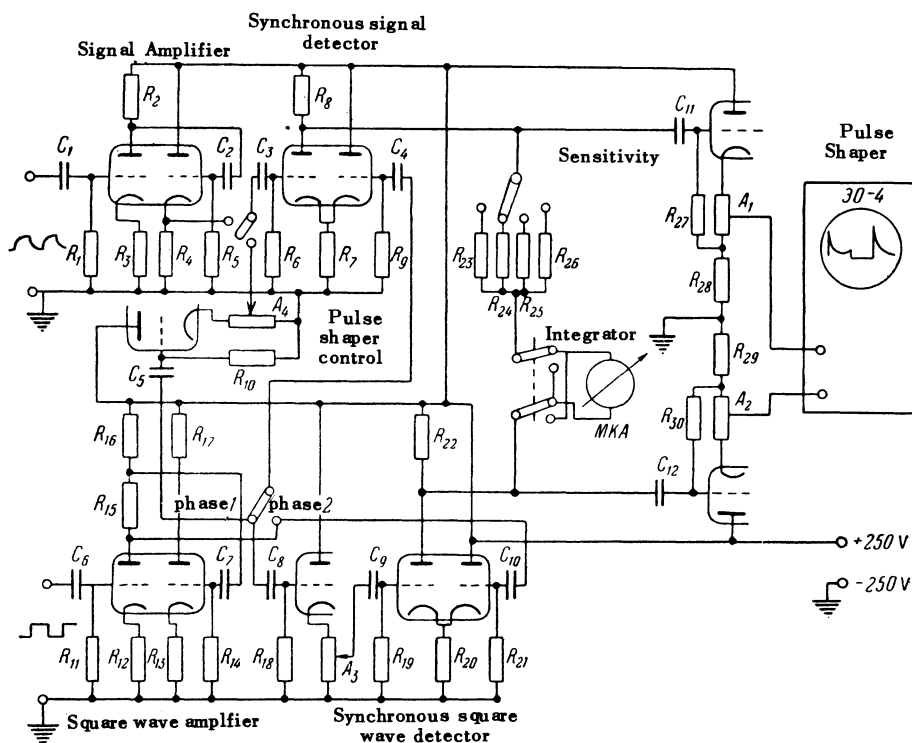


FIG. 8. Circuit diagram of the *L*-meter. All tubes are 6N8. *MKA*-microammeter with a shadow-type indicator; *EO-4*-cathodic oscilloscope.

$C_1, C_2, \dots, C_{14} = 4 \mu\text{F}$ .  $R_1 = 0.5 \text{ M}\Omega$ ;  $R_2 = 2.5 \text{ k}\Omega$ ;  $R_3 = 1 \text{ k}\Omega$ ;  $R_4 = 5 \text{ k}\Omega$ ;  $R_5 = 0.5 \text{ M}\Omega$ ;  $R_6 = 0.5 \text{ M}\Omega$ ;  $R_7 = 4.7 \text{ k}\Omega$ ;  $R_8 = 6 \text{ k}\Omega$ ;  $R_9 = 0.5 \text{ M}\Omega$ ;  $R_{10} = 0.5 \text{ M}\Omega$ ;  $R_{11} = 0.5 \text{ M}\Omega$ ;  $R_{12} = 2 \text{ k}\Omega$ ;  $R_{13} = 2 \text{ k}\Omega$ ;  $R_{14} = 0.5 \text{ M}\Omega$ ;  $R_{15} = 0.6 \text{ k}\Omega$ ;  $R_{16} = 1 \text{ k}\Omega$ ;  $R_{17} = 3 \text{ k}\Omega$ ;  $R_{18} = 0.5 \text{ M}\Omega$ ;  $R_{19} = 0.5 \text{ M}\Omega$ ;  $R_{20} = 4.7 \text{ k}\Omega$ ;  $R_{21} = 0.5 \text{ M}\Omega$ ;  $R_{22} = 6 \text{ k}\Omega$ ;  $R_{23} = 50 \text{ k}\Omega$ ;  $R_{24} = 0.2 \text{ M}\Omega$ ;  $R_{25} = 0.5 \text{ M}\Omega$ ;  $R_{26} = 1 \text{ M}\Omega$ ;  $R_{27} = 0.5 \text{ M}\Omega$ ;  $R_{28} = 4 \text{ k}\Omega$ ;  $R_{29} = 4 \text{ k}\Omega$ ;  $R_{30} = 0.5 \text{ M}\Omega$ .  
 $A_1, A_2 = 1 \text{ k}\Omega$ ;  $A_3 = 5 \text{ k}\Omega$ ;  $A_4 = 5 \text{ k}\Omega$

Figure 7 shows the block diagram of the *L*-meter, and Fig. 8 shows its circuit diagram. Note that the square wave amplifier is equipped with two outputs from which are derived the square waves controlling the operation of the two synchronous detectors. The square waves at these outputs are oppositely phased (phase 1 and phase 2, Fig. 8). When one of these phases is utilized, the rise curves are eliminated, and the *L*-meter integrates

the decay curves; when the other phase is utilized, the decay curves are eliminated and we obtain the areas above the rise curves.

## 6. CHARACTERISTIC CURVE OF THE *L*-METER

For the adjustment and testing of the *L*-meter, calibrated exponents of the form  $V = V_0(1 - e^{-t/\tau})$

("rise") and  $V = V_0 e^{-t/\tau}$  ("decay"), obtained as a result of the charging of capacitor  $C$  through the resistor  $R$  by square waves from a special square wave generator, were imposed on the input of the  $L$ -meter in place of the actual pulses to be investigated. Since we knew the values of  $V_0$  and  $\tau = RC$  beforehand, we could determine the areas  $L_p$  and  $L_z$  of our calibrated exponents and compare them with the areas  $L_p$  and  $L_z$  measured on the  $L$ -meter, and thus judge the accuracy of its operation. The areas  $L_p$  and  $L_z$  for the exponent are obviously equal.

$$L_p = -\tau V_0; \quad L_z = \tau V_0. \quad (3)$$

Thus the reading of the  $L$ -meter must be proportional to both  $V_0$  and  $\tau$ . Measurements showed that the dependence of the average current through the integrating unit on the magnitude  $\tau$  and the dependence of the average current through the integrating unit on the magnitude  $V_0$  (at  $\tau = 1.2 \times 10^{-4}$  sec) for both the "decay" curve and the "rise" curve are strictly linear (deviation from linearity less than 1%). The linearity of the characteristic curve of the  $L$ -meter is based on the linearity of all its stages; the frame of reference of this linearity is, of course, the limited range of input voltages employed in the  $L$ -meter. As a result of the control measurements, we determined that with input voltages which do not exceed 3 v the  $L$ -meter retains its linear characteristics. Since the amplitude of the pulses derived from the photoelectric multiplier does not exceed this value as a rule, and for the most part is ordinarily much lower, this input range is entirely satisfactory.

The readings of the integrating unit, aside from their linear dependence on  $V_0$  and  $\tau$ , must be directly proportional to the repetition frequency of the relaxation curves. For example, in studying the  $L_p$  and  $L_z$  of luminophors with the aid of the optical unit described in unit 4, the readings of the integrator will be proportional to the speed of revolution of the disc  $D$ , which modulates the light\*. Measurements have shown that the dependence of the strength of the current through the integrator on the speed of revolution of the disc is linear within the limits of accuracy of the measurement. The signals here were luminescence relaxation curves for uranyl potassium sulphate (exponents with  $\tau \approx 2 \times 10^{-4}$  sec).

The accuracy of operation of the  $L$ -meter thus

\* The constancy of the speed of revolution is controlled in our optical setup with the aid of a stroboscope using a neon lamp fed by a 50 cycle voltage.

depends on the repetition frequency of the signals, on their amplitude and on their speed of relaxation. In practice, it is possible to measure  $L_p$  and  $L_z$  for curves equivalent (in area) to exponents with  $\tau > 10^{-5}$  sec. As  $\tau$  is increased, the accuracy is increased; however, curves with too large a  $\tau$  ( $\gg 10^{-1}$  sec) will be distorted as a result of "low-frequency pile-up", introduced by the divider circuits.

The operation of the  $L$ -meter was tested on a series of luminophors with exponential relaxation (ruby, uranyl salts) and with well-known  $\tau$  values. The relationship of  $L_z$  and the relationship of  $L_p$  for these substances (at the induced brightness of luminescence) coincided well with the relationships of their  $\tau$ 's. However, measurements of  $L_p$  and  $L_z$  alone are of no slight interest for non-exponential relaxation curves. The present work does not have systematic measurements of this sort as its aim; however, as an important illustration, we present the results of measurements of the magnitude  $L_p/L_z$  for the phosphor ZnS-Cu (with a concentration of copper equal to 1%) at various temperatures.

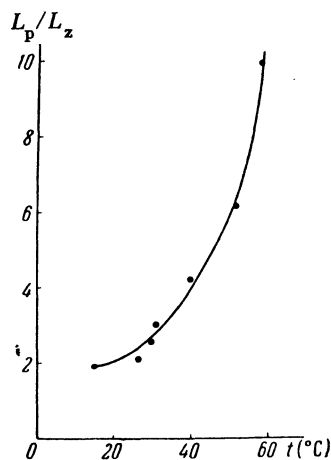


FIG. 9. Dependence of the ratio  $L_p/L_z$  on temperature for the phosphor ZnS-Cu (concentration of copper  $10^{-2}$  g/g).

The phosphor was placed in a transparent oven, the internal temperature of which was measured by a thermocouple. Excitation was produced by the mercury line  $\lambda = 365$  m $\mu$ . Figure 9 presents the graph of the dependence of  $L_p/L_z$  on temperature. As can be seen, the ratio  $L_p/L_z$  even at room temperature is equal to two (this conforms to the fact that the given phosphor is noticeably quenched

at room temperature); this ratio rises rapidly with temperature, attaining a value equal to 10 at a temperature of approximately 60° C.

From the considerations developed in Sec. 2, we became convinced of the fact that in the quenching of a phosphor with a bimolecular recombination mechanism, the ratio  $L_p/L_z$  must not exceed a value equal to three. The obvious nonfulfillment of this condition (Fig. 9) signifies the invalidity of the application of the usual bimolecular schematic to phosphors of the ZnS-Cu type, even under conditions of strong quenching when the mechanism of their recombination has indubitably been freed of complications to a very considerable degree. Note that the great difference between  $L_p$  and  $L_z$  ( $L_p \gg L_z$ ) is generally typical for quenched phosphors of the sulphide type. It is significant that even the introduction of the concept of the dependence of the probability of quenching on the intensity of the excitational

light<sup>5</sup> (the quenching action of excitational light) is unable to produce the result  $L_p/L_z \gg 3$ , since in the case

$$\beta = \beta_T + \beta_0 E$$

(where  $\beta$  is the total probability of quenching,  $\beta_T$  is the probability of purely thermal quenching,  $\beta_0$  is the probability of optical quenching and  $E$  is the intensity of the excitational light) the ratio  $L_p/L_z$  assumes a value of  $< 3$ .

$$L_p = 3I_0/(\beta_T + \beta_0 E); \quad L_z = I_0/\beta_T;$$

$$L_p/L_z = 3 \frac{\beta_T}{\beta_T + \beta_0 E} < 3.$$

<sup>5</sup> N. A. Tolstoi, Dokl. Akad. Nauk SSSR 95, 249 (1954).

Translated by A. Certner  
233